URTeC: 5297

Multi-Disciplinary Fracture and Spacing Study in the DJ Basin

Jason Brand*[1], Jessica Barhaug*[1], Roger Reinmiller[2], Ronald Parker [2], Bilu Cherian[3], 1. Great Western Petroleum, 2. Borehole Image Specialists, 3. Premier Oilfield Group.

Abstract

Despite having drilled thousands of horizontal wells into the Niobrara and Codell formations in the DJ Basin, the industry still hasn't settled on a preferred set of parameters for well spacing or frac design. Great Western Petroleum designed this project in 2019 to better characterize both natural and induced fractures in the formation, using an array of diagnostic tools across multiple disciplines.

We combined logging in both pre-completion unstimulated horizontal wells and post-completion fracture observation wells to characterize the natural fracture set and the induced hydraulic fracture set. After completion, we integrated geochemical analyses, pulse tests, and production surveillance techniques to study the dynamic connectivity between wells both within individual benches and between benches. Finally, we used a history-matched reservoir simulator to integrate as many data sets as possible into a single interpretation.

The hydraulic fracture network that was observed from the fracture observation wells was vast and dense. We observed over 1,400 hydraulic fractures and over 3,000 natural fractures on interpreted image logs that were run on the two wells. Notably these fracture sets were near perpendicular to each other suggesting a change in maximum principal stress between natural fracture formation and hydraulic fracture. As expected, we saw strong communication between wells based on all the data sets based on the spacing and frac design used. The different diagnostic data sets led us to similar conclusions, despite a wide range of data acquisition costs. We observed a high degree of vertical communication between the wells, but the communication between wells in the same bench was minimal. This trend continued over time with all the datasets as well. The strong interwell communication led us to adjust our well count, while taking frac volumes into account. We also calibrated the low-cost data sets for future work, which we began applying to new pilot projects in 2020. However, there were key difference between the different data sets that lead to important conclusions about the time-dependent behavior of inter-well communication.

This is the first time for these kinds of data sets to be integrated into a single publication, and the first time for several of these data sets to be published from the DJ Basin. Our work points to the possibility of inferring key reservoir characteristics from low-cost data sets like geochemistry, pulse tests, and basic production surveillance techniques with infrequent collection of high-cost datasets like post-frac logging. These low-cost datasets also have the advantage of minimal impact on operations. Our shut-in time for

pulse tests has been decreased to a few hours, while still providing quantifiable interwell communication. Additionally, we used the interpretations for this project to design future spacing pilots that we believe will substantially improve well economics.

This project was only possible through the collaboration across petrotechnical disciplines, from drilling engineering and geophysics as we drilled the FOW's, to petrophysics and geochemistry as we characterized the rock and fluid properties, to reservoir and production engineering as we analyzed pulse tests and monitored production performance. As the title suggests, this project could only have been achieved by a multi-disciplinary team.

Introduction

The unicorn of every oil producing basin is finding the optimal frac design paired with the appropriate well spacing. Many techniques are available to help in the search, with varying degrees of cost and success. This project took an approach that paired high-cost data acquisition with low-cost data acquisition to aid in getting closer to finding this elusive combination for the DJ Basin assets. By validating the low-cost data, these techniques could be used moving forward to analyze the effectiveness of future pad spacing and frac design.

The DJ Basin is a North-South trending asymmetric Laramide Foreland basin encompassing more than 70,000 square miles in Wyoming, Colorado and Nebraska. Oil and Gas development in the DJ Basin started with the discovery of the Florence Oil Field in Florence, CO in 1881. The Florence oil field produced from the Fractured Pierre formation which is sourced from the Upper Cretaceous Niobrara Formation. The Florence Oil Field is the oldest continuously producing oil field in the United States. Historical production in the DJ Basin comes from geological targets ranging in age from the Pennsylvanian through Upper Cretaceous and the basin has produced over 2 billion Barrels of oil and 11 TCF of gas since its inception in 1881.

The work discussed in this paper will focus on the Cretaceous Niobrara and Codell formations. The Codell formation is a low permeability sandstone deposited in a shallow marine environment and within the DJ Basin the Codell is unconformably overlain by the Niobrara formation. The Niobrara formation consists of interbedded organic-rich carbonates (chalks) and calcareous shales (marls). There are three horizontal drilling targets within the Niobrara that are designated as the A, B & C benches by most operators in the basin.

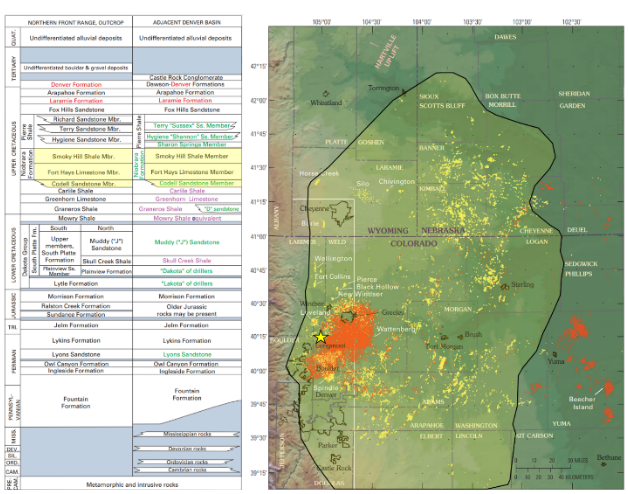

Figure 1. Stratigraphic Column of the DJ Basin on the left, representative of the map view of the DJ on the left. Science pad is designated with a yellow star. (After Higley and Cox, 2007)

Basin Development History
The Upper Cretaceous Niobrara and Codell formations were targeted heavily starting in the mid-1980's through vertical drilling and single stage fracing techniques. This drilling was as dense as 20 wells per section and up to 1999 had produced over 50MMBO & 550 BCFG, primarily from the West-Central part of the basin (Higley and Cox, 2007). In the late 90's & early 2000's, several lateral Niobrara completion attempts were made within the DJ Basin with limited success. In 2009, EOG drilled their Jake #2-01H lateral Niobrara well in NE Weld County, completed this well with a multi-stage completion and the well IP'd at over 1,500 BOPD. This set in motion the modern horizontal development of the Niobrara and Codell formations. Since 2008, the Niobrara and Codell horizontal play has produced over 1 billion Barrels of Oil & 5 TCF within the DJ Basin.

Over the next 12 years of development, operators have struggled to understand what the proper spacing of lateral wellbore development should be in order to maximize recovery factor while delivering acceptable returns to their investors. There has been a considerable amount of thought put in to modeling the different development approaches, including interwell spacing, completion fluid rheology and fluid and proppant volumes since modern development started in 2008. Operators have drilled between 1 & 30 wells per section, using slick water, hybrid and gel jobs, while experimenting with different proppant mesh sizes. During this same period, there has been very little data available in the public domain regarding direct measurements of interaction between the completed interval of horizontal development wells. Most investigations performed by operators were done through microseismic, where microseismic events were analyzed to locate stimulated rock or approximate the stimulated rock volume (SRV). Other investigations were centered around hydraulic fracture models where rock properties, frac volumes and fluid rheology were incorporated into simplified earth models to simulate the hydraulic and propped rock volume. While both approaches are industry standards for approximating SRV in unconventional resource development, direct observation of the fractured network was lacking from both.

Science Pad Background
The approach outlined here is an attempt to ground truth a physics-based Earth and hydraulic stimulation model using real-world observations of the hydraulic fracture network that was created in situ. These observations will then be used to constrain the modeled results in order to better understand the interwell communication within different modeled wine rack development scenarios. These 'intelligent' models will then be integrated with lower cost datasets to create a path forward for interpretating well spacing results at minimal cost.

The science pad is in western Weld County, just west of the Basin axis. In this area, all 3 benches of the Niobrara and the Codell are present and part of the horizontal development wine rack. This E-W oriented 1280-acre spacing unit has been developed vertically with 12 Niobrara and Codell wells that produced over 170MBO & 450MMCF between 2008 & 2018. In 2018, the vertical wells were plugged and abandoned, and a horizontal drilling campaign was used to drill 8 horizontal wells, equally distributed across the three Niobrara benches and the Codell. These wells produced over 700MBO & 1.7BCF between September 2018 and the commencement of this science project in June 2019. Both the vertical and horizontal production was contained to the N/2 of the spacing unit. There was only one vertical producer in the S/2 before the children wells were drilled.

Reservoir Characterization Methods

Fracture Observation (FO) Wells
The science presented in this paper is centered around a set of FO wells that were drilled through the wine rack after the producing wellbores were drilled and completed. The producing wells were put on flow back for approximately 2 months in order to reduce pressure post fracture treatment, then the offsetting producing wells were shut-in to prevent potential mud losses during drilling of the FO wells. The FO

wells were drilled for the sole purpose of data collection and have not been cased or produced. These wells were each designed to drill within approximately 50' of three different producing wells in an attempt to intersect as many hydraulic fractures as possible. In order to achieve this, the FO wells were drilled directionally across both horizontal and vertical planes. The Lo/Hi FO Well lands adjacent to a C-Bench producing well and climbs vertically at an average inclination of 94.7 degrees to intercept a B-Bench and A-Bench producing well as it traverses to the west southwest. The Hi/Lo FO Well lands adjacent to a B-Bench producing well and descends vertically at an average inclination of 86.7 degrees to intercept a C-Bench and Codell producing well as it traverses to the west northwest.

Both FO wells were drilled with water-based mud to allow sample collection for mineralogy, Source Rock Analyzer (SRA) and fluid inclusion investigations that would have been adulterated by oil-based drilling fluids. The water-based drilling mud also allowed us to acquire resistivity borehole image logs with a far greater resolution than image logs acquired from oil-based drilling fluids. Both FO wells have approximately 1-mile lateral sections. Rock cutting samples were collected at 100' increments along both FO laterals which results in a sample collected every 10' of TVD change on average. Both FO Laterals were logged with full triple combo data in order to calibrate the cuttings mineralogy to the earth model.

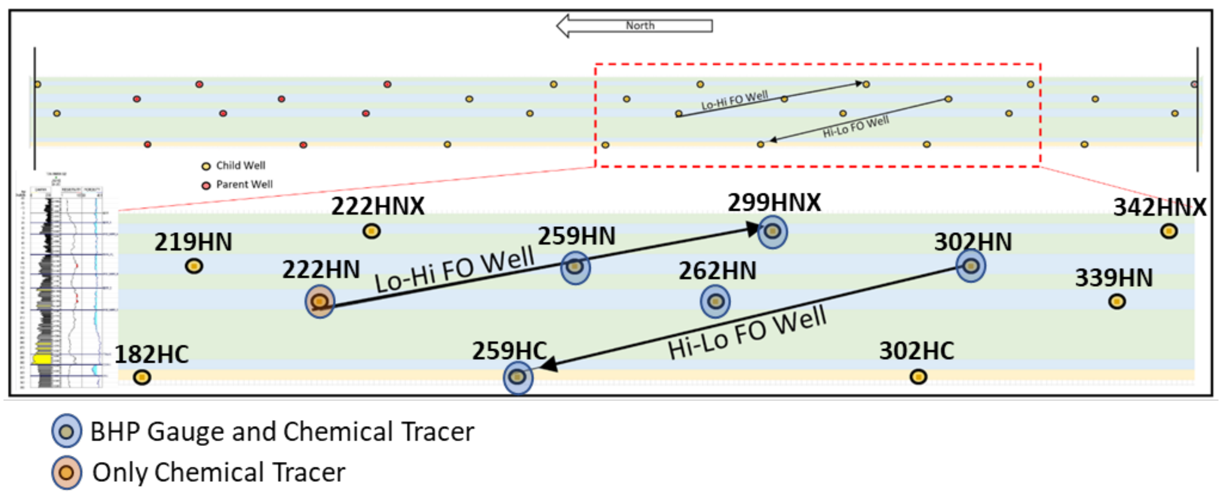

Figure 2. Wine rack depicting the location of the FO Wells, bottomhole pressure (BHP) gauges and wells where chemical tracer was pumped during the completions with type log for reference. Zero vertical exaggeration.

The pad was developed using 2016 vintage 3D Seismic data for structural control and geosteering decision making. The 3D volume shows a large ~75'-deep graben complex trending roughly N-S approximately 1.5 miles west of the landing point. This structure was confirmed through the drilling of the producing wellbores. The FO wells were intentionally drilled within the easternmost mile of the development to avoid this graben complex and the influence such a large structural feature might have upon hydraulic fractures from our wine rack. This graben feature intersects all producing wellbores and has implications for the well interference test discussed later in this paper.

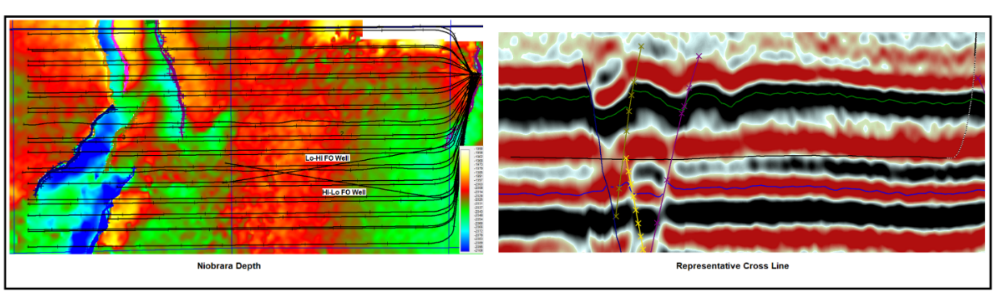

Figure 3. Niobrara Depth Map and Cross Line showing location of Graben relative to FO wells and Production Wells.

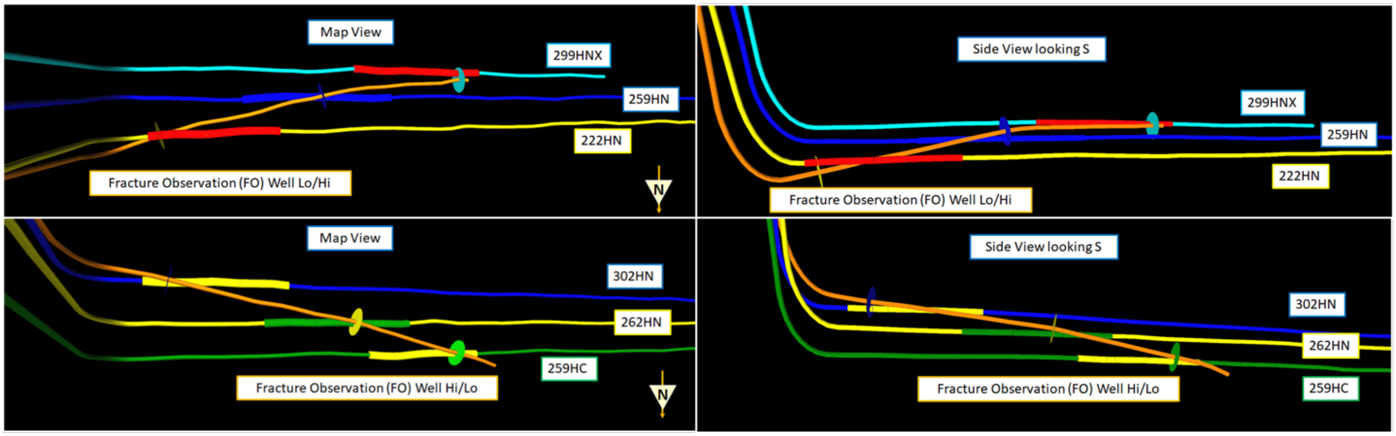

Figure 4. Map and side views of the lateral clusters for the Lo/Hi FO well (upper pair) and the Hi/Lo FO well (lower pair). The Lo/Hi well rises from the C Marl up to the A Chalk where it then becomes horizontal. The Hi/Lo FO well cuts at a low-angle downward from the A Chalk to the B Marl, and then steepens as it passes down to the Codell. The discs along the FO wells indicate points of closest approach to the laterals.

Image Log Acquisition

Three types of image log data were collected. The 6 production laterals with image logs were drilled with oil-based mud (OBM). Image data were acquired from these wells using a PetroMar FracView, Logging-While-Drilling (LWD) acoustic imaging tool. Two of the 6 OBM laterals were also run with a Compact Oil-Base Mud Microimager (COI). Image data from the FO wells were collected by a Compact MicroImager (CMI) in water-based mud (WBM). The three image log acquisition methodologies have different sensitivities. OBM tools have diminished resolution compared to WBM tools. As an acoustic tool, the LWD operates by measuring variation in sonic velocities. Features that display good impedance contrast, such as lithological changes and open fractures, are well resolved. Features with low impedance contrast, such as cemented fractures, are not resolved. The OBM resistivity tool is able to resolve open and cemented fractures but cannot differentiate them (OBM in open fractures resembles resistive, cemented fractures). The WBM tool offers the best feature resolution, permitting identification of open, partially-open, and cemented fractures.

Static Model

Key to understanding development drivers is characterizing petrophysical properties, textural properties, and stress state. A petrophysical model was initially constructed using a triple combo dataset with core data (saturations, porosities, grain-density, XRD volumes and Leco TOC). 8 wells were utilized within the study area to build a triple combo model. Cuttings analysis performed on the study wells further constrained the mineralogy, providing confidence in the porosity and saturation results. The petrophysical model was then applied to 14 wells within the science pad section and an additional 76 wells within the seismic section. 90 wells and the seismic horizons aided in defining the framework model. A seven facies model was created using the mineralogical curves (Bentonites, Argillaceous Mudstones, Silty Sandstones, Marls, Chalks, Limestones). The porosity, permeability and saturation were modeled with a facies bias. Saturation was co-simulated with the previous porosity.

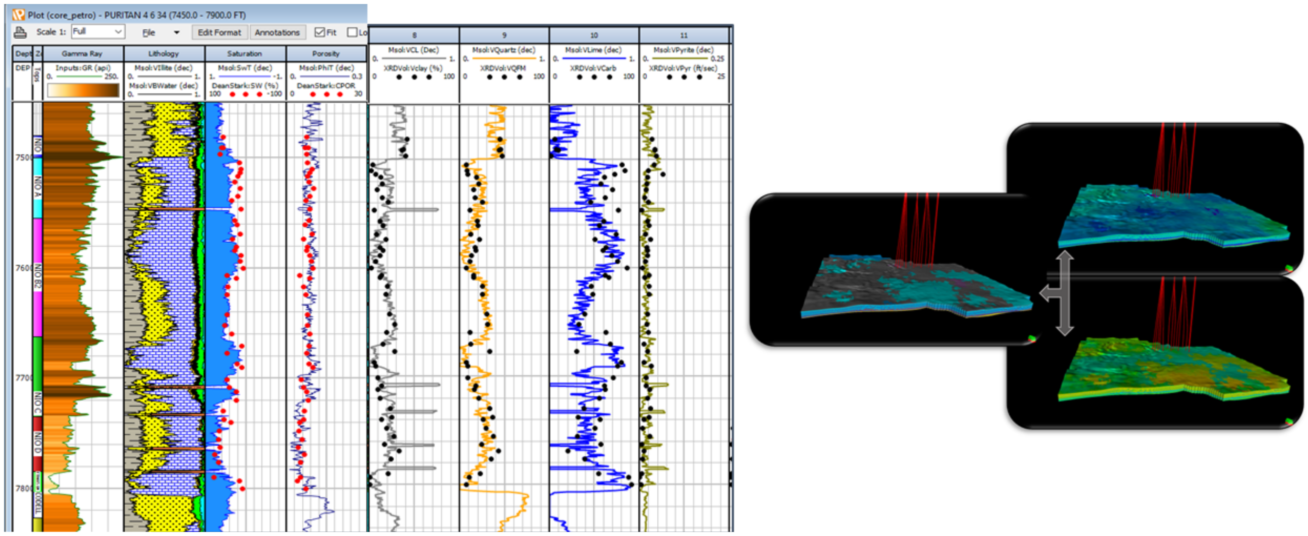

Figure 5.Petrophysical model matching core applied to multiple wells to create static model

A Mechanical Earth Model (MEM) was constructed to understand hydraulic fracture propagation in the study area. Rock mechanical properties and total and effective far-field stresses were computed using nearby sonic data and core data to aid in fracture modeling. Offset bottomhole pressures and DFITs constrained pore-pressure within the Niobrara/Codell horizons. Where uncertainty existed (shallower and deeper horizons), a variable pore pressure ramp profile was created by carefully evaluating various log signatures. Fracture pressure history matching was utilized as a tool to constrain geomechanical uncertainties together with the diagnostic data gathered on the pad. The zero-lateral strain-based Ben Eaton model was utilized to derive anisotropic stresses using elastic properties by integrating variable Biot-poro-elastic constants, pore pressure estimates, overburden, azimuthal mechanical properties and tectonic loading. Effective stresses provided constraints on confining stresses for porosity-permeability relationships and pore-pressures and ramps (validated by fracture modeling and tracer data) provided constraints to reservoir simulation (history matching).

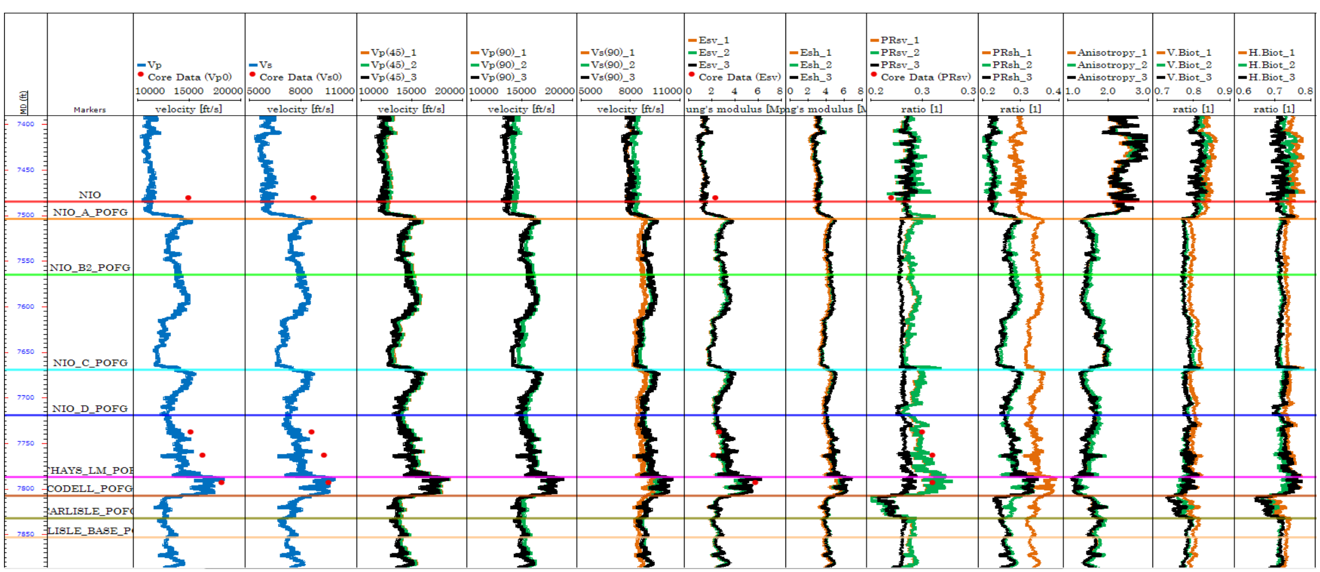

Figure 6. Building of geomechancial model – calibration to core data

Engineering Methods

The main objective of the engineering data was to evaluate well spacing. Surveillance data from recent tighter wine racks pointed to well interference. The science pad included a variety of datasets to compliment surveillance techniques. The datatypes, and the methods used to gather them, are detailed below. Key to understanding stacking, staggering, and spacing is determining system permeability and fracture dimensions. A significant amount of data was compiled (seismic, logs, cores,) to characterize the subsurface (stress, petrophysical and textural properties) and an equally extensive set of data was collected (tracers, pulse tests, image logs, geochemical fingerprinting) to characterize hydraulic fracture lengths and fracture heights as a function of producing time.

Geochemical fingerprinting

Cuttings were used to establish oil type by geochemical composition for the chalk and marl components of all three Niobrara benches, for the Fort Hays Limestone and for the Codell Sandstone. With these baseline oil types, oil samples collected from different production intervals could be used to fingerprint interference between wells over time. Parent and children wells were sampled three times (Figure 7).

Geochemical	Chemical Tracer	Interference Test
Nov. 27th 2019	Aug. 20th 2019	Dec. 5th-12th 2019
Dec. 27th 2019	Oct. 2nd 2019	Feb. 19th - 27th 2020
Feb. 14th 2020	Feb. 4th 2020	

Figure 7. Sampling Schedule of the Different Datasets

Chemical Tracers

36 unique oil soluble and 36 unique water-soluble tracers were pumped on 6 children wells to examine fracture hits (water tracer) and the long-term connectivity between well pairs (oil tracer). The same tracer was pumped across 3-4 stages in a well in order to see what sections of the lateral were in communication with offset producers (Figure 8).

222HN			259HN			299HNX			259HC			262HN			302HN		
Stage #	Water Tracer	Oil Tracer	Stage #	Water Tracer	Oil Tracer	Stage #	Water Tracer	Oil Tracer	Stage #	Water Tracer	Oil Tracer	Stage #	Water Tracer	Oil Tracer	Stage #	Water Tracer	Oil Tracer
18			18			18			18			18			18	10275	15110
19			19			19			19			19			19	10275	15110
20			20			20			20			20			20	10275	15110
21			21			21			21			21			21	10275	15110
22			22			22			22			22			22	10475	15190
23			23			23			23			23			23	10475	15190
24			24			24			24			24			24	10475	15190
25			25			25			25			25			25	10475	15190
26			26			26			26			26			26	10250	15040
27			27			27	2500	15000	27			27			27	10250	15040
28			28			28	2500	15000	28			28			28	10250	15040
29			29			29	2500	15000	29			29			29	10250	15040
30			30			30	2500	15000	30			30	1000	15750	30	10175	15160
31			31			31	2800	15070	31	3900	15550	31	1000	15750	31	10175	15160
32			32			32	2800	15070	32	3900	15550	32	1000	15750	32	10175	15160
33			33	1900	16700	33	2800	15070	33	3900	15550	33	1000	15750	33	10175	15160
34			34	1900	16700	34	2800	15070	34	3900	15550	34	1100	15010	34	10200	15800
35			35	1900	16700	35	2900	15350	35	4000	16650	35	1100	15010	35	10200	15800
36			36	2000	16350	36	2900	15350	36	4000	16650	36	1100	15010	36	10200	15800
37			37	2000	16350	37	2900	15350	37	4000	16650	37	1100	15010	37	10200	15800
38	10450	15200	38	2000	16350	38	10375	16250	38	4000	16650	38	1200	15600	38	3000	16450
39	10450	15200	39	2000	16350	39	10375	16250	39	4000	16650	39	1200	15600	39	3000	16450
40	10450	15200	40	2100	15150	40	10375	16250	40	2400	15650	40	1200	15600	40	3000	16450
41	10450	15200	41	2100	15150				41	2400	15650	41	1200	15600	41	3000	16450
42	10750	16000	42	2100	15150				42	2400	15650	42	1300	15170	42	3700	16400
43	10750	16000	43	2100	15150				43	2400	15650	43	1300	15170	43	3700	16400
44	10750	16000							44	2400	15650	44	1300	15170	44	3700	16400
45	10750	16000							45	10100	15700	45	1300	15170	45	3700	16400
46	2200	16150							46	10100	15700	46	1500	16550	46	10400	15850
47	2200	16150							47	10100	15700	47	1500	16550	47	10400	15850
48	2200	16150							48	10100	15700	48	1500	16550	48	10400	15850
49	2200	16150										49	1500	16550	49	10400	15850
50	2300	16050										50	1400	15050	50	10225	15400
51	2300	16050										51	1400	15050	51	10225	15400
52	2300	16050										52	1400	15050	52	10225	15400
53	2300	16050										53	1400	15050	53	10225	15400
54	10325	16100										54	1600	16200			
55	10325	16100										55	1600	16200			
56	10325	16100										56	1600	16200			
57	10325	16100										57	1600	16200			
58	10925	15140										58	1700	15210			
59	10925	15140										59	1700	15210			
60	10925	15140										60	1700	15210			
61	10925	15140										61	1700	15210			
62	10425	15020										62	10125	16600			
63	10425	15020										63	10125	16600			
64	10425	15020										64	10125	16600			

Figure 8. Chemical tracers pumped by stage. Colored by tracer number.

The traced wells had the highest sampling rate, especially at the beginning of flowback and production. The offsets were sampled three times to look at interwell communication (Figure 7).

Interference/Pulse Tests

A workflow has been established to analyze well pairs and to calculate the magnitude of pressure interference (MPI) in each direction. This effort builds on the work conducted by Chu et al (2018) based on the Chow Pressure Group (CPG) methodology, which was originally published in 1952. To calculate the MPI, a well is shut-in for a number of hours and then allowed double the recovery time before the next well is shut-in. If an increase in pressure is seen at the time of the shut-in on an offset well, then a decline curve is extrapolated to fit what the offset pressure would have been. This difference in pressure can then be used to calculate the MPI.

$$\frac{\Delta P}{2 * \frac{d\Delta P}{dt}}$$

where, ΔP is the change in pressure and $\frac{dP}{dt}$ is the derivative of ΔP with respect to time.

A weak well-to-well connection is considered anything less than 0.5, moderate is 0.5-0.75 and strong is above 0.75. Two rounds of interference tests were performed to see any degradation of interwell connectivity over time. In addition to examining interference between wells, the first round was also used to optimize the shut-in time across different benches. The goal was to obtain a quantifiable measure of interference across a set of wells with minimal disruptions to operations. To accomplish this, the shut-in time was varied across the wine rack to see the minimal shut-in required to observe a pressure pulse. Shut-ins varied from two up to nine hours. A shut-in was performed on all of the children wells on the pad. The shut-in order was randomly distributed across the wine rack, ensuring ample recovery time. Identifying pulses via surface pressure can be challenging, so BHP gauges were placed in 5 of the wells. The second round used the optimized shut-in times that were derived from the initial tests.

Surveillance Techniques

Several surveillance techniques that were applied to previous pads were used at the science pad to determine how they compared to the science pad. This allowed for comparison to the previously described datasets, as well as, to surveillance data already analyzed from offset producing pads.

1. Rate Transient Analysis
   a. RTA was conducted on all of the parent and children wells at the science pad. Standard Productivity Index (PI)-cum plots were used to estimate EUR.
2. BHP Trends
   a. Extended shut-ins for the drilling of the FO wells occurred on all five of the wells with a BHP gauge installed. This allowed for analysis of the shut-in period.

Reservoir Simulation

Extensive fluid testing had been performed in the DJ to characterize fluid properties. A black oil model was used to capture observed Rsi of 1,450 scf/stb and Psat of 3,100 psi. Mercury injection capillary pressure data was analyzed to define relative permeability curves for the key facies (Marls/ Chalks). Yilmaz-Nur correlation was used to fit experimental data published by Cui, Q (2016). Public domain permeability data was utilized to create permeability relationships per facies. A fine grid (5 ft x 10 ft x 10 ft) reservoir model was extracted from the geo-model. Grids were rotated (NNE-SSW) to align with the principal stress direction assumed from the image logs. Fracture geometries generated from fracture pressure history matching the hydraulic fracture treatment were used to capture the propped fractures. Local Grid Refinement (LGR) captured the hydraulic fractures obtained from fracture pressure history matching (constrained to diagnostics gathered).

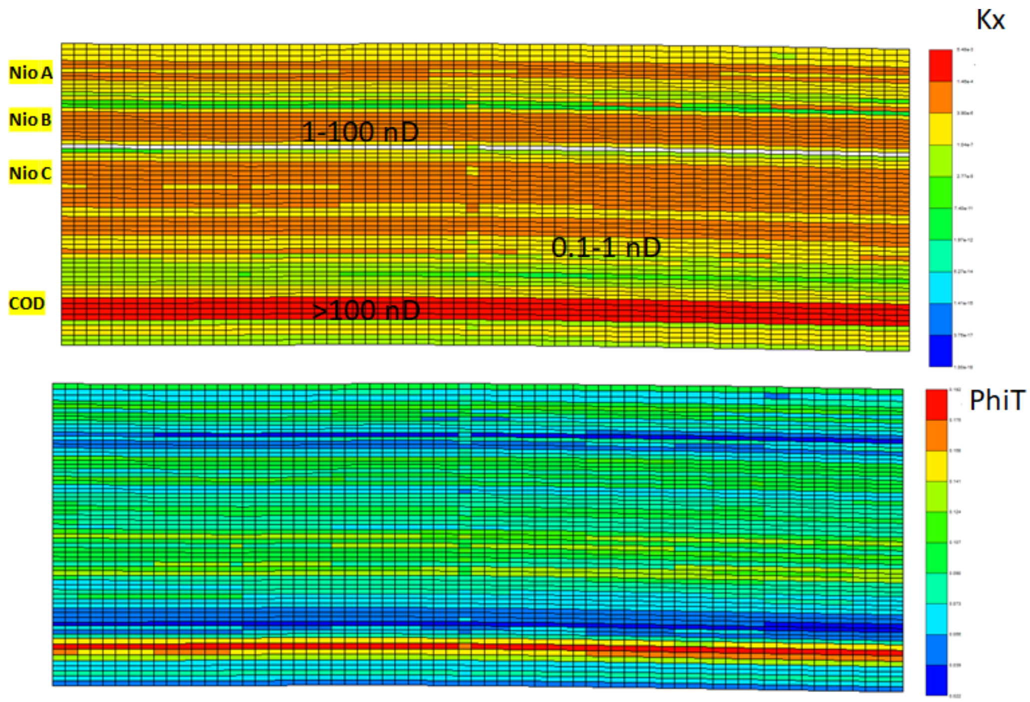

Figure 9. Reservoir simulation model

Reservoir Characterization Results

Analysis and interpretation of borehole image log data from the 6 laterals and the 2 FO wells were aimed at establishing the spatial geometry of the natural fractures in all 8 wells and to characterize the fractures produced by hydraulic stimulation. The results of the image log fracture analyses are summarized in the 4 lower-hemisphere, equal-area stereonet diagrams in Figure 10 and Figure 11.

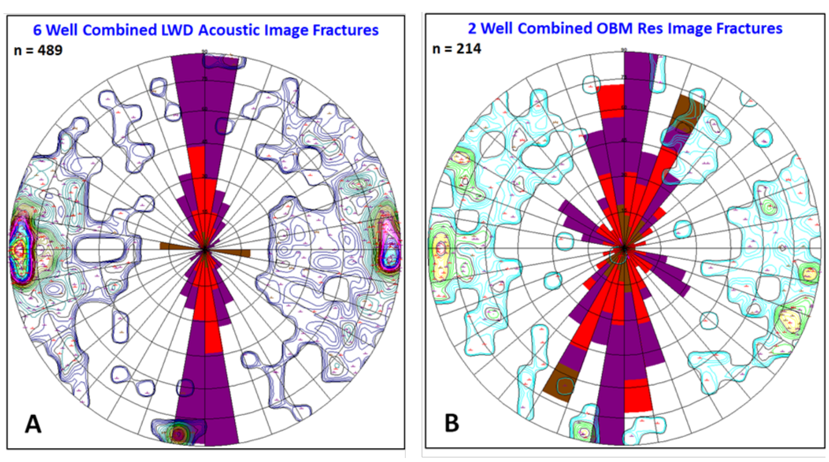

Figure 10. A: This shows the spatial geometry of the 489 natural fractures from the acoustic LWD image logs from the uppermost 5,000' of the 6 laterals. B: This diagram compiles the 214 fractures measured from the OBM resistivity tool from 2 wells.

Figure 10A compiles fractures mapped from the LWD Acoustic image tool run in the 6 laterals. These fractures display a N-S strike trend, dipping at high-angles to the E and W. Most of these fractures are partially-open (purple), with fewer closed fractures (red). The paucity of cemented fractures (pink) reflects low-impedance contrast of this fracture type to an acoustic image tool. Cemented fractures are likely present but are invisible to the acquisition device. Figure 10B combines the fracture data from the

OBM resistivity images acquired from 2 of the laterals (222HN and 302HN). With a greater degree of scatter, a N-S strike trend is still dominant. Like the LWD acoustic data, these fractures are comprised of open, partially-open and closed features. The paucity of cemented fractures (pink) reflects the low sensitivity of oil-based mud (OBM) resistivity tools to this type of feature. Hence, they may be present, yet undetected.

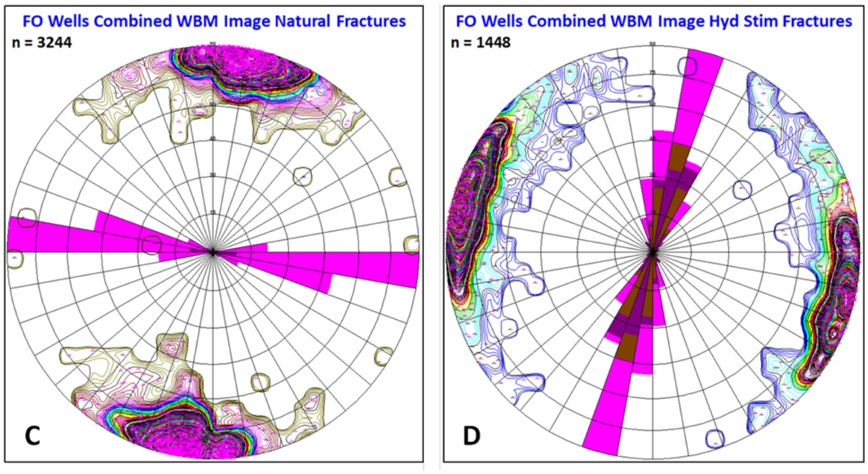

Figure 11. These are fracture strike diagrams of NFs (C) and HSFs (D) compiled from both FO Wells.

Figure 11C compiles the 3244 Natural Fractures from the 2 FO wells. These features are almost entirely cemented fractures (pink) and they are extremely well resolved by the WBM tool (Figure 12). These natural fractures display a tightly-constrained strike trend with maxima oriented slightly clockwise of E-W and dipping at high-angle to both the N and S.

Figure 11D summarizes the spatial geometry of the 1448 hydraulic stimulation fractures (HSFs) identified from both FO wells. The HSFs display a strong strike trend, oriented NNE-SSW and dipping at high-angle to both the WNW and ESE. The NNE-SSW strike trend of the HSFs is interpreted to be the orientation of the maximum horizontal compressive stress (SHMax). This interpretation is supported by alignment with recently published SHMax data in the vicinity of the science pad (Lund Snee, 2021).

Most HSFs appear as resistive (pink) features, and this presents a conundrum. Under normal circumstances, HSFs in image logs appear as conductive (dark) features because newly-opened apertures are filled with conductive WBM. Resistive fractures (pink) in WBM are usually interpreted as cemented. Mineral fill in HSFs prior to image log acquisition is improbable. One explanation for resistive HSFs is that they are filled with hydrocarbons. Before FO well installation, the 6 laterals were producing oil. The FO wells were then drilled through the SRV that, in previous months, was conducting fluid transport. Thus, resistive HSFs may reflect reservoir drainage that was “caught in the act” - a highly unusual scientific observation.

The HSF strike trend is interpreted to align with SHMax. Considering that the angle between the NF and HSF strike maxima is ~80°, it is probable that hydraulic stimulation would not be able to reactivate the natural fracture set and this is supported by the image logs in the FO wells.

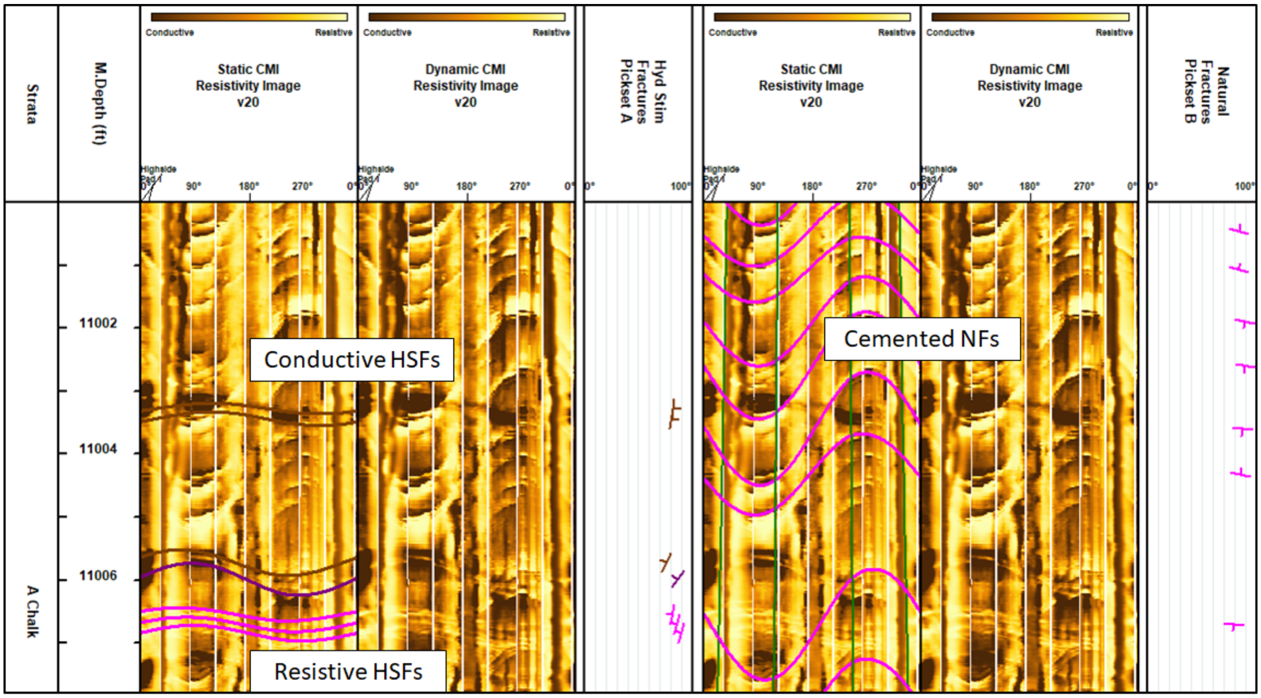

Figure 12. This snapshot displays the different appearance of Hydraulic Stimulation Fractures (HSFs) and Natural Fractures (NFs) from the A Chalk of the Lo/Hi FO well. HSFs appear as full sinusoidal traces that occur in discrete swarms of 2-5 subparallel cracks. HSFs have open apertures aligned with SHMax (N-S) and are typically filled with drilling fluid. In the case of WBM this fluid is conductive (dark). That some HSFs have resistive (pink) aperture fill suggests that these HSFs might have been "caught-in-the-act" of draining oil from the producing reservoir. NFs, in contrast, are high-angle, mineral-filled parallel breaks that have a regular spacing and an E-W strike.

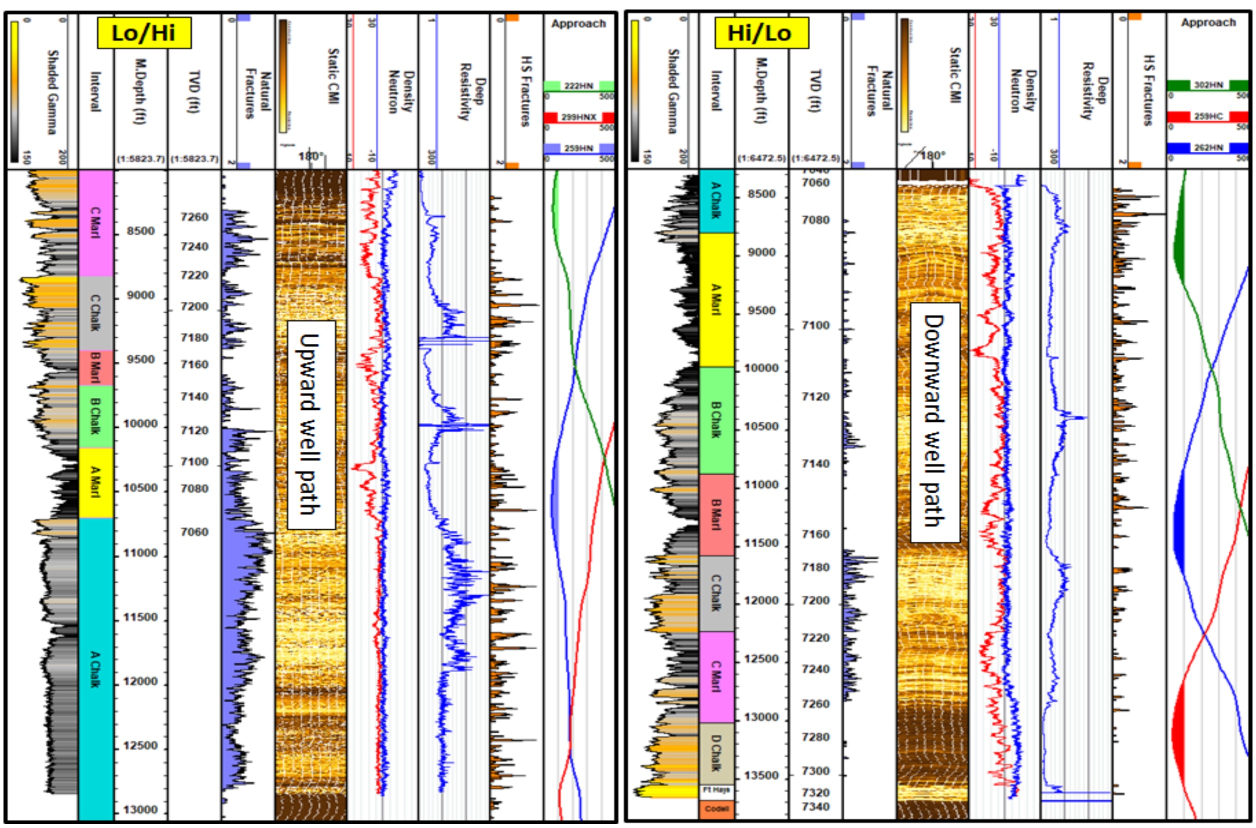

Figure 13. These figures compare open hole logs and NF and HSF frequency curves against the closest approach curves for the two FO wells.

The closest approach curves, scaled 0 to 500', measure the position of the corresponding FO wellbore as it nears, and then departs, the labeled lateral. The approach curves are shaded when the separation distance is less than 100'. The Lo/Hi FO well crosses laterals 222HN, 259HN and 299HNX; the laterals transected by the Hi/Lo well are 259HC, 262HN and 302HN. The Hi/Lo NF frequency curve displays many fewer fractures than are seen in the Lo/Hi well, likely reflecting the difference in A Chalk length. Although HSFs are expected to increase in abundance with proximity to a stimulated lateral, this is not apparent except for the 302HN curve (Hi/Lo, green). In fact, closest approach is associated with diminished HSF frequency in the case of the 259HC (Hi/Lo, red) and the 222HN (Lo/Hi, green). These relationships suggest other dominant controls, such as lithology or rheology.

The image log component of this study was able to establish the spatial geometry and distribution of fracture types within the 6 laterals and the 2 FO wells. Natural fractures are dominated by cemented features striking ~E-W (from WBM) and partially-open and closed features striking ~N-S (from OBM). Fractures induced by hydraulic stimulation occur in clusters and strike to the NNE-SSW, in alignment with SHMax. Anomalously, a high proportion of HSFs are resistive, suggesting that image logs from the FO wells captured a snapshot of a reservoir being actively drained. The high angle (~80°) between SHMax and the cemented natural fractures suggests that they would not be reopened by hydraulic stimulation, as indicated by the image log in the FO wells.

Static Model

Water saturation computed from Petrophysical logs and calibrated to core agree with water cuts produced from the well. Permeabilities obtained from the public domain proved to be the key uncertainty. History match permeabilities (>50 nD for Niobrara and greater than 100 nD for Codell) agreed with values reported within literature (Ning, 2017; Cui 2016; Tanner et al, 2019; Rosenhagen et al, 2019) and were 10-fold smaller than Byrnes et al (2018). Hydraulic fractures inserted into the static model via LGR agreed with image log observations of approximately one fracture every 8 ft. The observation of orthogonal natural fractures and close long hydraulic fractures and the observation of faulting connecting the wellbores of multiple wells created two possible hypotheses for well connectivity detected in the pulse tests/geochemical fingerprinting.

Engineering Results

Geochemical Fingerprinting

Figure 14 displays a wine rack layout of the oil typing results by well. The first row of the wine rack contains the results from the Niobrara A wells. The oil being produced from the A bench wells is mainly A Chalk oil with some wells containing some A Marl, B Chalk and Marl and C Chalk and Marl. Out of all the benches, the A wells contain the most oil from the targeted bench. Over time, some wells began to include more A bench oil, but others like the 059HNX and the 342HNX saw a decrease in A bench oil contribution by the third round of sampling.

For the B bench wells, there was increased variability in the oil types. One of the more interesting wells is the 022HN, a parent well. During the first round of sampling, the majority of the oil type found was from the A Chalk. Over the next two rounds, more B bench oil returned, but ~25% of the oil is still from the A bench. The 302HN, 219HN and 142HN all began producing more B bench oil over time, whereas the 259HN had a majority of B bench oil from the onset.

The Niobrara C wells have the most variability of all the benches. Due to their proximity both laterally and vertically to A bench locations, all the wells had at least 25% A bench oil during the first round of testing. Most of the wells saw this initial A bench oil type decrease over time, however, 062HN (a parent well), 339HN and 222HN saw increases in A bench contribution before a decrease during the final round of sampling. B bench oil was also detected in all of the C bench wells with the 382HN seeing a large increase in B bench contribution during the third sample.

For the Codell wells, most saw a gradual increase in Codell oil contribution over time. The other oil types that were most prolific in the Codell wells came from the Ft. Hays and the C bench. Very little B bench oil and no A bench oil was found in the Codell. Some wells (379HC and 259HC) saw a decrease in Codell contribution during the second round of testing but had more Codell oil detected during the final test. The oil type geochemical fingerprinting shows that oil from different benches is apparent at all benches of the wine rack (minus A to Codell and vice versa). Shared drainage between the wells is alive and well, even over the 6-month sampling period.

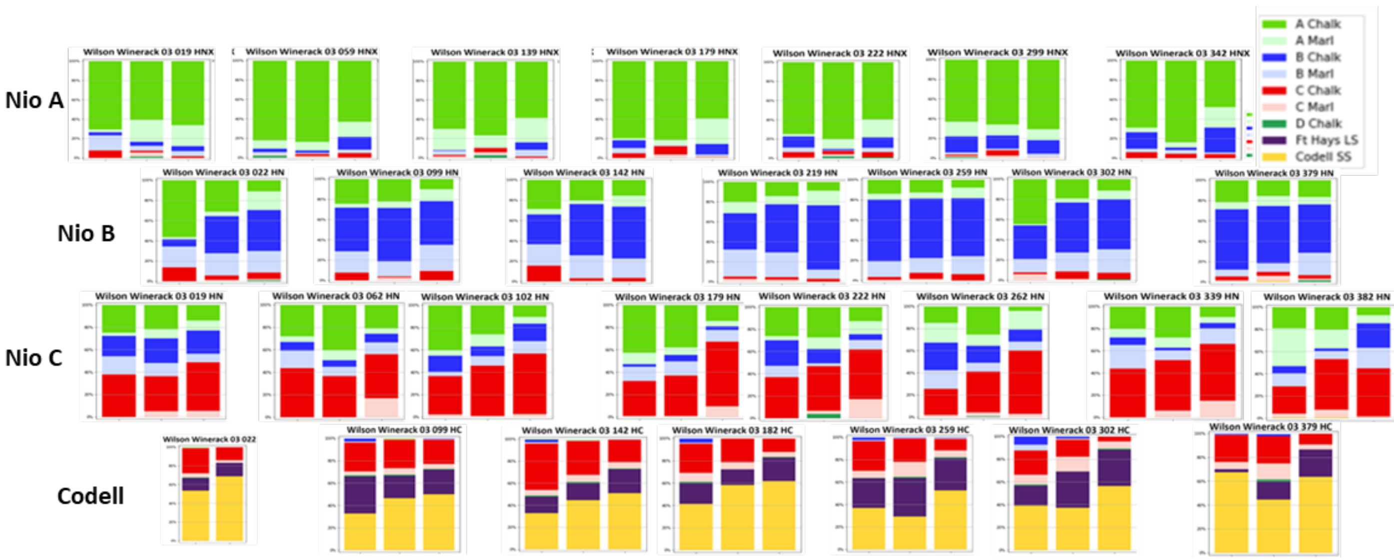

Figure 14. Geochemical fingerprinting results displayed by sample date on the x axis (refer to Figure 7 for exact dates) and percent contribution by oil type (colors shown in the legend) on the y axis. The wells results are positioned by location in the wine rack.

Chemical Tracers

Similar to the geochemical fingerprinting, the chemical tracers showed significant communication between the wells. The water-soluble tracers pumped in the 6 wells were detected in the first offsets, second offsets and even some of the parent wells. The oil tracers were more confined but still detectable in some offsets. 299HNX (the sole A bench traced well) saw offset water tracers in the 262HN (direct offset C bench well) and the 302HN (direct offset B bench well), but not much detectable anywhere else. This communication carried over to production with oil tracers present in the 262HN and 302HN. However, the amount of oil tracers pumped into the 299HNX versus oil tracers detected in the treatment well and the offsets is disproportional. The lack of detectable oil tracers indicates that the fracs broke up into the Sharon Springs and have since closed, leaving the tracer stranded.

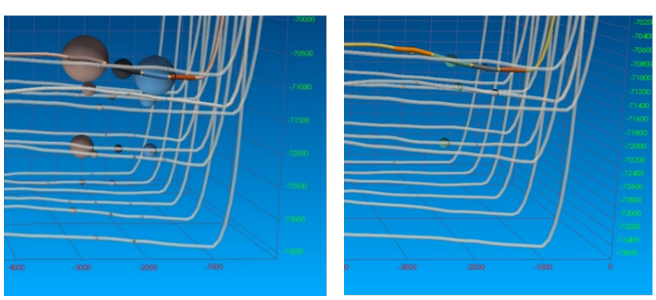

Figure 15. Side view of the chemical tracer results on the 299HNX, with the water tracers on the left and oil tracers on the right. The type of tracer pumped is shown along the lateral of the 299HNX, with the different colored sections. The corresponding colored spheres are sized by amount of tracer detected. This is representative of the last round of sampling for the treatment well and all of the offsets.

The first water tracer pumped on the 259HN B bench well, in stages 33-35, was detectable in every sampled well, except for the 302HN, its direct B bench offset. The majority of oil tracer from this stage was present in the treatment well and not in the offsets. The other tracers pumped in this well only had minimal signatures in offset wells. In the 302HN, the water tracer pumped in stages 34-37 was found in high concentrations in the offset wells, but water tracers from other stages were also apparent. Most of the water tracers appeared in wells to the east of the 302HN with only scarce amounts in the 259HN. The oil tracers were not present in most of the offset wells and there were only two stages where detectable amounts were present in the treatment well during sampling.

For the water tracers pumped in the directly offset C bench wells, 262HN and 222HN, the 262HN water tracer was detected across all benches to the west of the 262HN, even down to the two Codell parent wells (099HC and 022HC). The only water tracer detected to the east of the 262HN was a small amount in the 302HN B bench first offset. This well had the most offset oil tracer seen of any well with strong communication from most stages to the 259HN, 299HNX and the 302HN. The strongest communication was observed with the 259HN. When examining the 222HN, the direct C bench offset, a greater degree of containment was observed during frac. There was a small amount of upward growth to the 219HN, but the majority of offset water tracers were found in all the Codell wells minus the 379HC. No water tracers were detected in any of the wells to the east of the 222HN. The oil tracers had moderate concentrations in the 182HC, 219HN and trace amounts in the 099HC parent well.

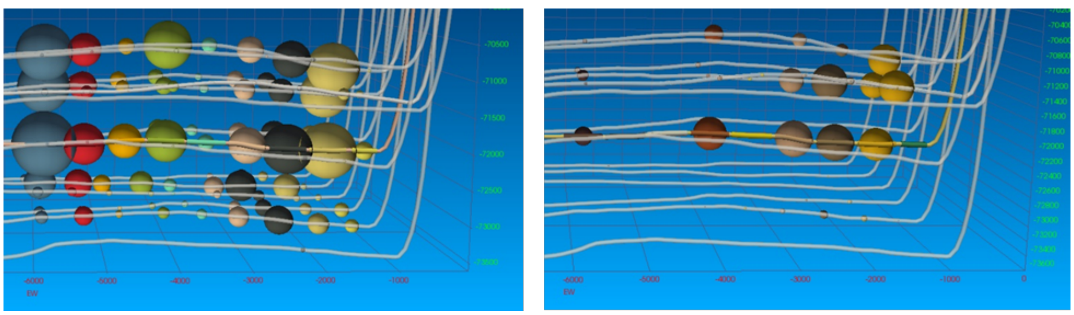

Figure 16. Side view of the chemical tracer results on the 262HN, with the water tracers on the left and oil tracers on the right. The type of tracer pumped is shown along the lateral of the 262HN, with the different colored sections. The corresponding colored spheres are sized by amount of tracer detected. This is representative of the last round of sampling for the treatment well and all of the offsets.

The sole Codell well with tracer was the 259HC. The water tracers in stages 40-44 had the highest communication with the Codell, Niobrara B and Niobrara C offsets. The water tracers from the other stages also saw communication across these same intervals, just not as prominent as the water tracer pumped in stages 40-44. Not much water tracers made it up to the A bench wells. The oil tracers saw communication with the 182HC (direct Codell offset) and slight amounts detected in the direct Niobrara B and C offsets.

Interference Tests

Both rounds of pulse testing were analyzed by well pair to look at the MPI from the shut-in well to the observation well and then vice versa. From analyzing the shut-in periods in round one, the conclusion was made that a four-hour shut-in is adequate for Codell wells and a six-hour shut-in is the minimum time required to observe an offset pressure pulse for Niobrara wells. This test also confirmed the necessity for double the recovery time (eight hours for Codell wells and 12 hours for Niobrara wells) before shutting in the next well. Figure x shows the MPIs from round one and from round two. The wells within the interior of the wine rack display a high-level of connectivity. However, this connectivity is limited to wells in other benches, as no wells show a connection laterally. The 262HN, 259HN and 299HNX all demonstrate high MPIs in both directions to their vertical offsets.

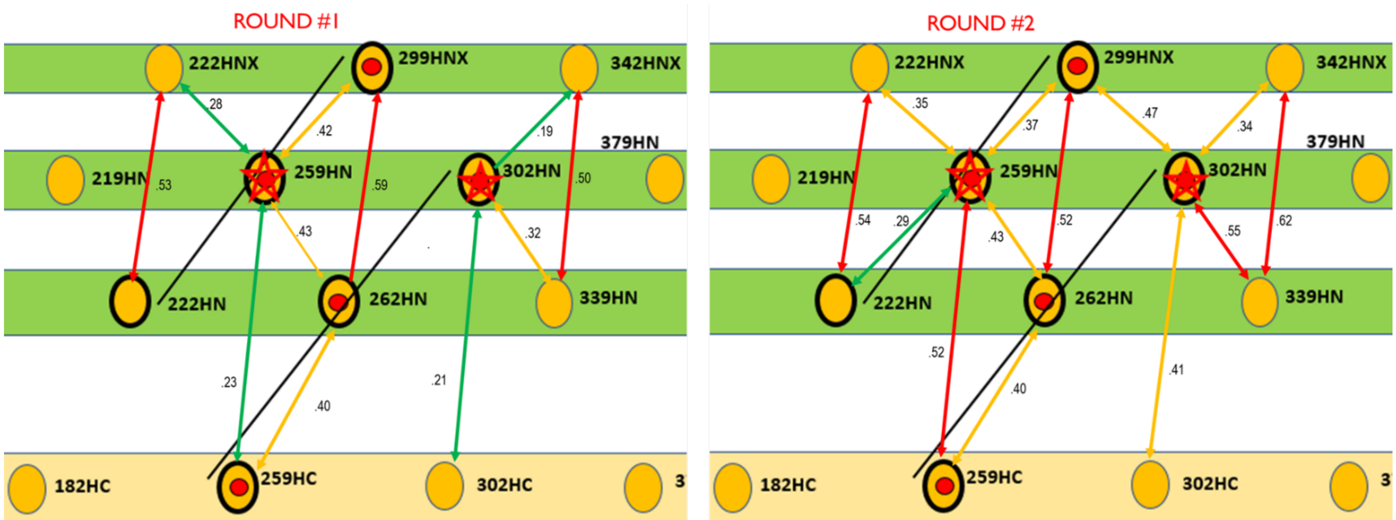

Figure 17. MPI Values from both rounds of interference tests. The MPI is the average between the observed MPIs from the well pair. A green arrow indicates an MPI between 0.2 and 0.34. A yellow arrow is a MPI between 0.35 and 0.49 and red is indicative of a MPI 0.5 or greater.

Surveillance Techniques

The RTA for the parent wells looked "typical", consistent with experience on offset pads. There were not noticeable slope changes on the PI-cum plot pre-frac hit and then some degradation of EUR was observed. The children wells saw this loss in EUR without even experiencing a frac hit; they incurred some very rapid, very strong changes in PI-cum that correspond to offset well behavior. Because of the strong interwell communication between the children wells, reserves were lost based on the new predicted EURs. Figure 18 displays an example of these drastic slope changes, from the 259HN, which had to be shut-in prior to the drilling of the FO wells. When the well was turned back on, the slope was much steeper, leading to a loss in reserves on this well.

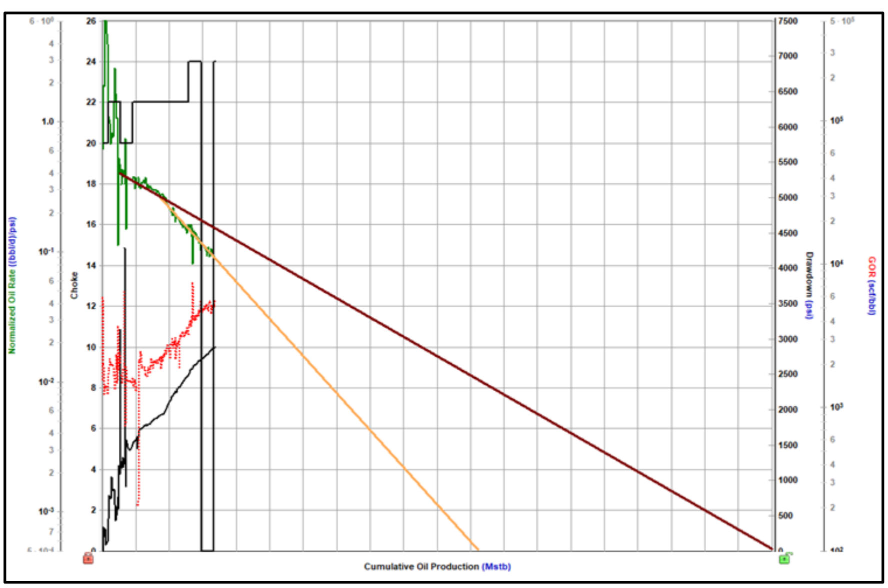

Figure 18. Normalized oil rate versus cumulative oil production for the 259HN. The choke size is on a secondary y axis, along with drawdown and GOR on their own separate axes. The maroon and orange trendlines highlight the PI-Cum slope change before and after the shut-in for the drilling of the FO wells.

The BHP gauges provided a unique dataset during the shut-ins for the drilling of the FO wells. After an initial pressure buildup, the pressures began to decline after a couple of days. This dataset also confirmed the connectivity of these fully-bounded wells.

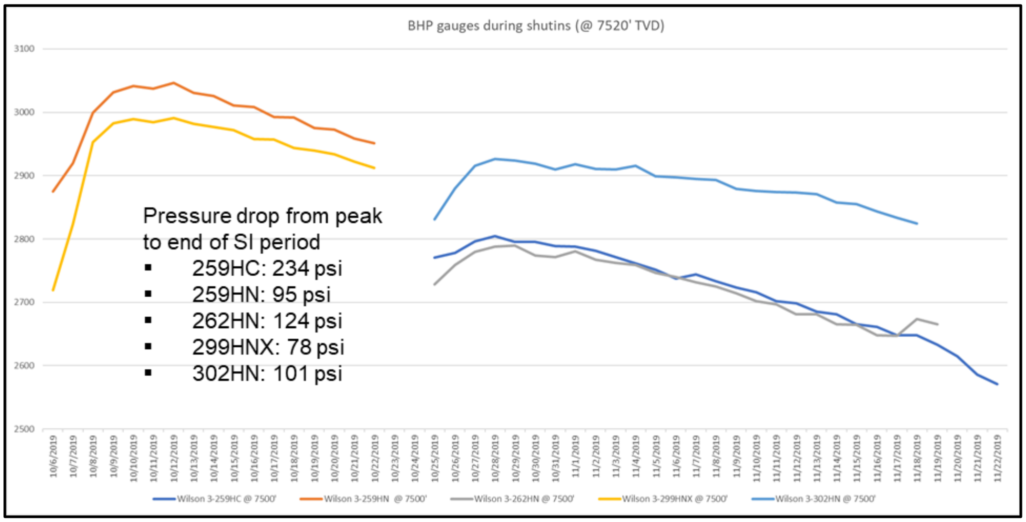

Figure 19. BHP values during shut-ins for drilling of FO wells

Reservoir Simulation

Fracture pressure history matching was performed using the geomechanical properties generated from sonic logs. Image logs and tracers confirmed long hydraulic fracture lengths. Fracture modeling indicated hydraulic heights of approximately 300 ft and lengths of up to 1,200 ft. With fractures observed almost every 8 ft, an interesting observation was the lack of stress shadowing. A hypothesis that the natural fracture / fault "network" could be activated by the hydraulic fracture treatment fractures to aid communication across wells is supported by the pulse tests (showing different degrees of communication as a function of vertical offset distance which relates to the geomechanics and hydraulic fracture modeling) and geochemical tracers (showing vertical communication). Fracture geometries were provided to reservoir engineering for simulation. Geomechanics and fracture modeling confirm significant vertical height growth. Uncertainty introduced into the study centered around the lack of constraints on local core permeability data. When public domain permeabilities (Smith et al, 2014 and Byrnes, 2018) were used, fracture geometries had to be significantly smaller than what fracture modeling

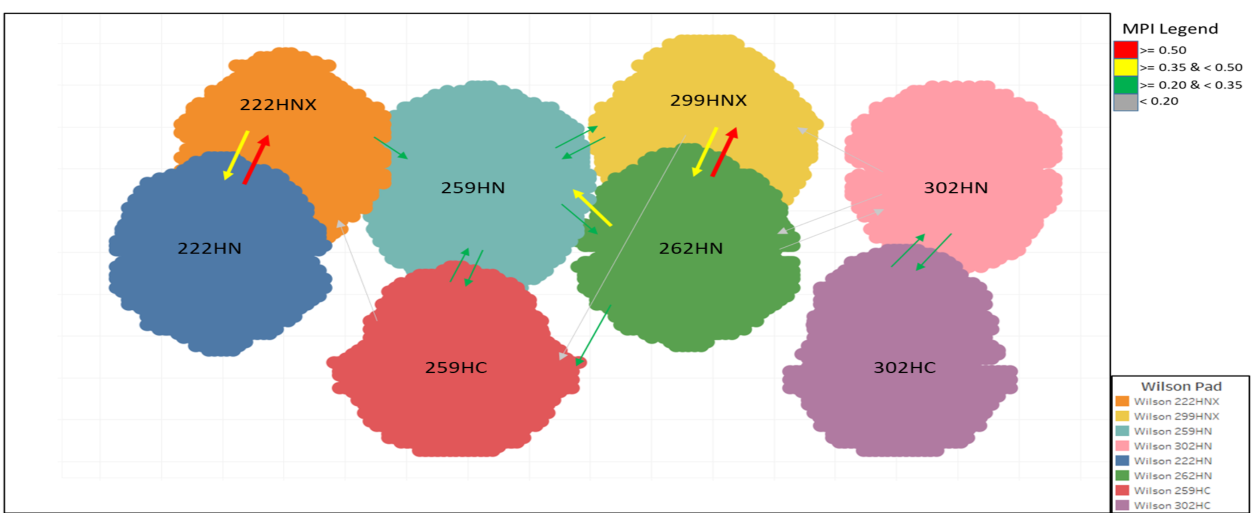

Figure 20. Hydraulic fracture clouds derived from fracture pressure history match combined with pulse test results.

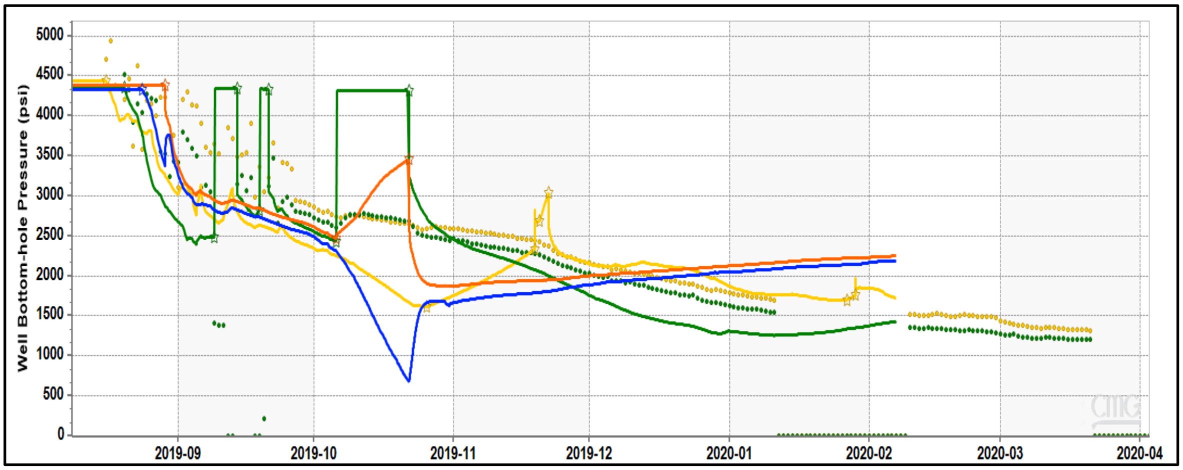

Figure 21. Reservoir simulation struggles to match pulse tests when high core perms are used and fracture modeling lengths are violated (made shorter)

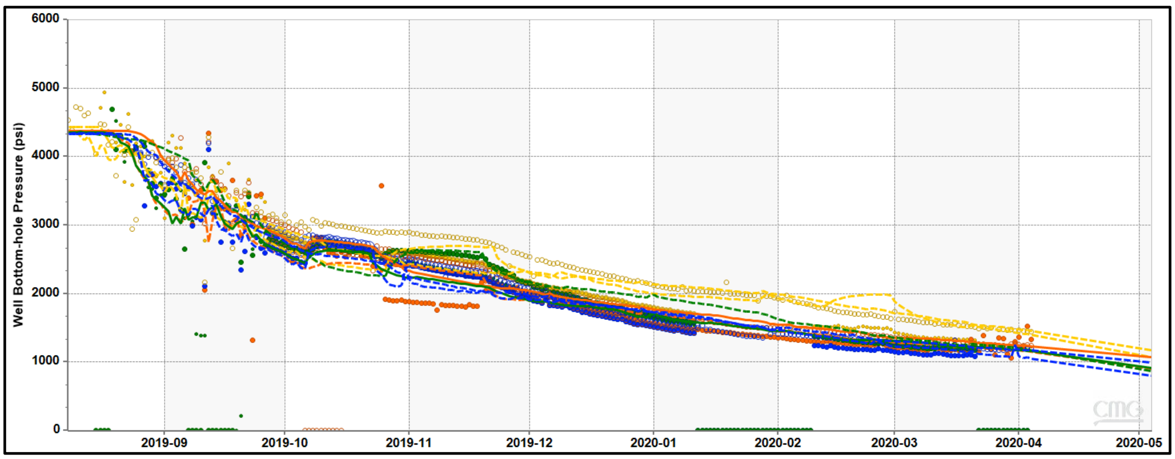

Figure 22. Reservoir simulation match pulse tests and geochemical tracers when lower perms (consistent with literature) and fracture modeling length are honored (creating connection pathways across wells)

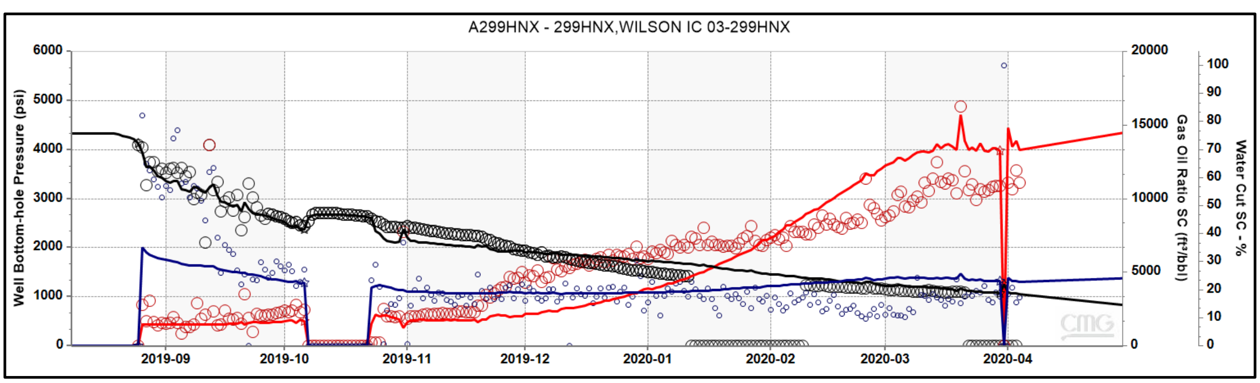

Figure 23. History match example on a well showing matching of pulse tests (slight increase in pressure is observed due to communication with a flowing well), water cuts and GORs.

suggested. This made it difficult to match the pulse tests and to honor the geochemical fingerprinting data. Reduction in permeabilities (<70 nD for Niobrara) resulted in longer productive lengths and heights which helped matching the pulse tests. The vertical connection of fracture (from fracture pressure history matching) also matches the gas segregation observed on this pad, where the shallower wells were gassier, and the deeper wells collected more water. Vertical communication was also confirmed by geochemical tracing. The use of numerical models enabled quantification of the MPIs. For high MPIs, up to 25% of the well was communicating with laterals in other benches, whereas for the moderate values, only 10% of the well was in communication.

Discussion

Once history matches were obtained, forecasting was performed to understand development strategies. Forecasts indicate that co-development can be challenging in the current spacing configuration due to the significant vertical communication. This could result in vertical asymmetry and poor in-fill length generation. Interference tests, oil tracers, geochemical fingerprinting and RTA also showed a high-level of vertical communication with not much degradation over time. It is difficult to determine what percentage of this communication is associated with the fracs versus faulting, but a pathway for communication is present.

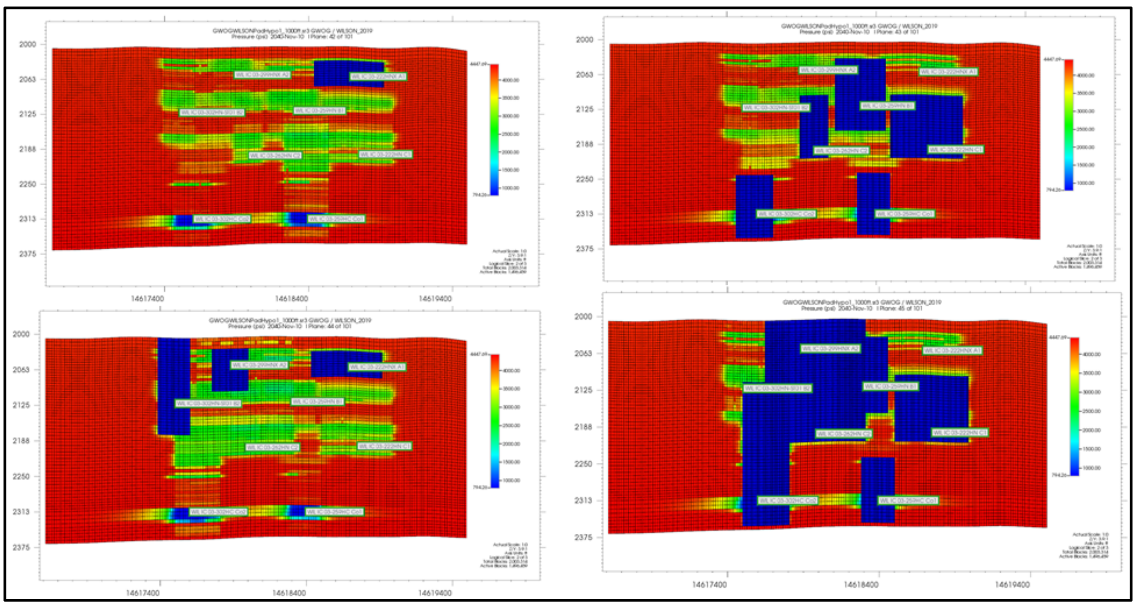

Figure 24. Reservoir Simulation Results Showing Depletion Profiles Overlapping Vertically

The results seen with the lower cost engineering data confirmed what was seen in the higher cost datasets (FO wells, image logs and reservoir simulation). Using pulse tests, RTA and frac modeling where vertical mechanical logs exists, combined with occasional geochemical fingerprinting and chemical tracer collection, the implications of changing well spacing can be analyzed. This isn't the 100% answer, but it's close enough to provide a level of confidence in interpretating adding or dropping wells from the wine rack at a fraction of the cost.

Conclusions

1. The decision was made to drop wells from the wine rack based on the well-to-well interference observed across the datasets. The quantification of the interference attributed to the HSF network is complicated by the large graben complex that intersects all producing wellbores. The dropping of wells will improve well and section level economics on future development.
2. Lower cost datasets were validated with the higher cost counterparts.

3. The fracture models are based largely on earth modeling that lacks the resolution to incorporate localized natural fracture variability.
4. Natural (NF) and hydraulic stimulation fractures (HSF) were well-resolved by image data with dominant strike trends oriented ~E-W and ~NNE-SSW, respectively. NFs are cemented and occur ~80° to SHMax, suggesting low reactivation potential. Resistive HSFs may preserve hydrocarbon drainage from a SRV.
5. The observed HSF network does not fit entirely with the fracture network inferred from the modeling work as the observed HSF network did not increase in frequency with proximity or calcite percentage as the models predict. This does not suggest a flaw in the model as these observations are affected by a multitude of operational and geological variables.

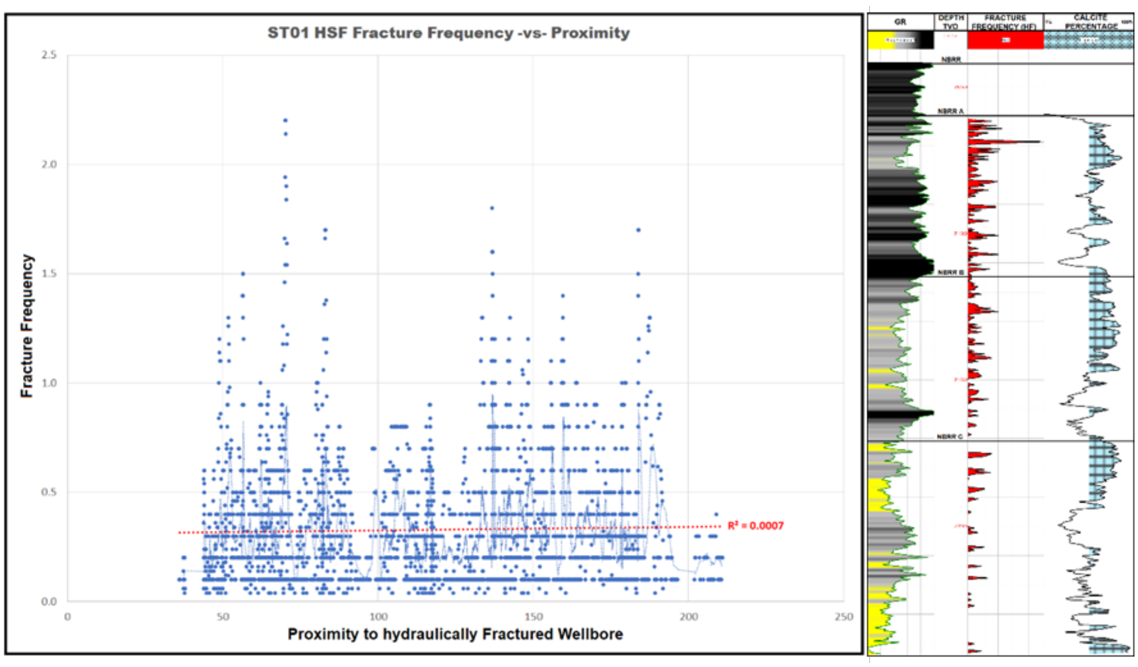

Figure 25. Cross plot of Hydraulic Fracture Frequency vs Proximity to Stimulated Wellbore Showing lack of correlation. TVD Log display comparing Percent Calcite to Hydraulic Fracture Frequency showing lack of correlation.

Acknowledgements

This project could not have been accomplished without unwavering dedication from multiple folks across a variety of disciplines. From the GWP Board of Directors that approved the project to the pumpers that collected samples and to everyone in between, this project would not have been possible without their contributions. On the Great Western side, special thanks to Zack Warren, Sarah Compton, Damon Parker, Willis Wilcoxon, Dana Hanneman, Ty Woodworth, Michael Andrews, Matt Mount and Gary Shinabarker. We'd also like to thank Scott Stinson, Faye Liu and Mike Mayerhofer for their contributions.

References

Byrnes, A., Zhang, S., Canter, L. and Sonnenfeld, M. 2018. Two-phase and three-phase relative permeability of unconventional Niobrara chalk using integrated core and 3D image rock physics. DWLS, 2018

Chu, W., Scott, K., and Fumerfelt, R. 2018. A New Technique for Quantifying Pressure Interference in Fractured Horizontal Shale Wells. Presented at the SPE Annual Technical Conference, Dallas, TX, 24-28, February. SPE-191407-MS

Cui, Qi. 2016. Stress Dependent Compaction in Tight Reservoirs and its Impact on Long-Term Production. thesis submitted to the Faculty and the Board of Trustees of the Colorado School of Mines in partial fulfillment of the requirements for the degree of Doctor of Philosophy

Higley, D. and Cox, D., 2007, Oil and gas exploration and development along the front range in the Denver Basin of Colorado, Nebraska, and Wyoming, in Higley, D.K., compiler, Petroleum systems and assessment of undiscovered oil and gas in the Denver Basin Province, Colorado, Kansas, Nebraska, South Dakota, and Wyoming—USGS Province 39: U.S. Geological Survey Digital Data Series DDS–69–P, ch. 2, 41 p.

Lund Snee, Jens-Erik, 2021, Crustal Stress and Geodynamics webpage, https://www.jenseriklundsnee.com/ Accessed 5/25/2021.

Smith, K., Bottjer, R., Sterling, R., Nowak, H., and Wheat, D. 2014. Reservoir Characteristics of the Codell Sandstone Tight Oil Play, Northern DJ Basin, Wyoming and Colorado: Extension of Wattenberg into the Oil Window, Search and Discovery Article #20262